

## Electron Raman scattering in asymmetrical multiple quantum wells

This article has been downloaded from IOPscience. Please scroll down to see the full text article.

2005 J. Phys.: Condens. Matter 17 4451

(<http://iopscience.iop.org/0953-8984/17/28/005>)

View [the table of contents for this issue](#), or go to the [journal homepage](#) for more

Download details:

IP Address: 129.252.86.83

The article was downloaded on 28/05/2010 at 05:37

Please note that [terms and conditions apply](#).

# Electron Raman scattering in asymmetrical multiple quantum wells

R Betancourt-Riera<sup>1</sup>, R Rosas<sup>1</sup>, I Marín-Enriquez<sup>2</sup>, R Riera<sup>2</sup> and J L Marín<sup>2</sup>

<sup>1</sup> Departamento de Física, Universidad de Sonora, Apartado Postal 1626, CP 83000, Hermosillo, Sonora, Mexico

<sup>2</sup> Departamento de Investigación en Física, Universidad de Sonora, Apartado Postal 5-88, CP 83190, Hermosillo, Sonora, Mexico

Received 17 May 2005

Published 1 July 2005

Online at [stacks.iop.org/JPhysCM/17/4451](http://stacks.iop.org/JPhysCM/17/4451)

## Abstract

Optical properties of asymmetrical multiple quantum wells for the construction of quantum cascade lasers are calculated, and expressions for the electronic states of asymmetrical multiple quantum wells are presented. The gain and differential cross-section for an electron Raman scattering process are obtained. Also, the emission spectra for several scattering configurations are discussed, and the corresponding selection rules for the processes involved are studied; an interpretation of the singularities found in the spectra is given. The electron Raman scattering studied here can be used to provide direct information about the efficiency of the lasers.

## 1. Introduction

In recent years, there has been considerable interest in asymmetrical multiple-quantum-well systems, because many new optical devices based on intersubband transitions are being developed. This feature could fulfil the need for efficient sources of coherent mid-infrared radiation for application in several branches of science and technology, such as communications, radar, optical electronics. For example, an intersubband Raman laser can be built with a three-level system [1–4], in such a way that the required energy between the levels can be obtained using a double or triple asymmetrical quantum well. These devices are made with epitaxially grown GaAs/Al<sub>x</sub>Ga<sub>1-x</sub>As,  $x$  usually around 0.35, and InGaAs/AlInAs [5]. The system consists of two or three asymmetric GaAs wells separated by GaAs/Al<sub>x</sub>Ga<sub>1-x</sub>As barriers [6]. Also there are works in which the second-harmonic generation in a quantum cascade laser for this kind of system is studied [7]; these processes are qualitatively too different to the phenomena that we are studying in this paper.

It is important then to study such systems in order to determine their properties, and thus properly predict their behaviour. Raman scattering is an ideal tool for this study, because of its precision in the optical characterization of nanomaterials. The electronic structure

of nanostructures can be studied through Raman scattering processes considering different polarizations of incident and emitted radiation [8, 9]. This is the reason that Raman scattering experiments are a powerful tool for the investigation of semiconductor nanostructures.

In this work, we present a model of electron Raman scattering (ERS) in asymmetrical coupled multiple (double and triple) quantum wells, where an electron in the conduction band of the first well undergoes an intersubband transition to a new energy level of the same well, if the system is an asymmetrical double quantum well (ADQW), or a corresponding one to the second well, if the system is an asymmetrical triple quantum well (ATQW), absorbing a photon of energy  $\hbar\omega_l$  (pump radiation); after that, the electron emits a photon of secondary radiation of energy  $\hbar\omega_s$  (laser radiation) carrying out an intersubband transition to the last quantum well, which is of several widths [1–3].

The model used to obtain the electronic envelope functions and energy levels presents little limitation, and the use of this model in the design of very precise and reliable laser devices is common practice today; furthermore, the techniques for growing semiconductor nanostructures allow the construction of quantum wells that present little, if any, difference from an ideal quantum well structure [10].

There exist works in which the authors have presented simulations of an optically pumped intersubband Raman laser realized in an artificial three-level system [11] using the density matrix method with the object of showing that the Raman gain is not proportional to the external pumping intensity. In our calculations it is not possible to obtain these results because we used a one-particle model; however, we provide the theoretical framework needed to calculate the condition for and efficiency of a tunable intersubband Raman laser, obtaining the corresponding analytical expressions.

## 2. Electronic states

The problem of finding the stationary states of an electron in the envelope function approximation in asymmetrical multiple-quantum-well systems leads us to solving the equation

$$\left\{ \nabla^2 + \frac{2m^*}{\hbar^2} [E_n - V(z)] \right\} \Psi = 0, \quad (1)$$

where  $m^*$  is the electron effective mass.

Let us now consider an asymmetrical multiple quantum well of rectangular shape grown along the  $z$ -direction, where the origin of coordinates is located at  $l_1$ , with  $2i$  interfaces located at  $z = l_1 = 0$ ;  $z = l_2 = d_1$ ,  $z = l_3 = l_2 + b_1$ ,  $z = l_4 = l_3 + d_2$ ,  $\dots$ ,  $z = l_{2i-1} = l_{2i-2} + b_{i-1}$ ,  $z = l_{2i} = l_{2i-1} + d_i$ ,  $i$  being the number of coupled wells and  $i - 1$  the number of interior barriers. The widths of the wells are  $d_i$ , with  $d_0 = 0$ , and the widths of the barriers are  $b_i$ . The height of the potential barrier  $V(z)$  and the effective masses  $m_i^*$  are given by

$$V(z), m_i^* = \begin{cases} V_0, & m_1^*, & z < l_1 \\ 0, & m_2^*, & l_1 \leq z \leq l_2 \\ \vdots & \vdots & \vdots \\ 0, & m_i^*, & l_{2i-1} \leq z \leq l_{2i} \\ V_0, & m_1^*, & l_{2i} < z. \end{cases}$$

The solution to equation (1) for  $i$  coupled asymmetrical quantum wells is formed of  $2i + 1$  envelope wavefunctions of the form

$$\Psi = \frac{\exp[-i\mathbf{k}_\perp \cdot \mathbf{r}_\perp]}{(L_x L_y)^{1/2}} \begin{cases} A_1 \exp(\gamma_n z) + B_1 \exp(-\gamma_n z), & z < l_1 \\ A_2 \cos(k_n z) + B_2 \sin(k_n z), & l_1 \leq z \leq l_2 \\ \vdots & \vdots \\ A_{2i} \cos(k_n z) + B_{2i} \sin(k_n z), & l_{2i-1} \leq z \leq l_{2i} \\ A_{2i+1} \exp(\gamma_n z) + B_{2i+1} \exp(-\gamma_n z), & l_{2i} \leq z \end{cases} \quad (2)$$

where  $k_n^2 = \frac{2m_n^*}{\hbar^2} E_n$  and  $\gamma_n^2 = \frac{2m_n^*}{\hbar^2} [V_0 - E_n]$ .

By considering the continuity of  $\Psi$  and  $(1/m_j^*)(\partial\Psi/\partial z)$  at all the interfaces we can calculate the constants  $A$  and  $B$  and the energy levels. In this work we are particularly interested in semiconductor ADQW and ATQW, mainly because they are currently used in the construction of infrared laser devices, which are made considering three levels in the conduction band.

The explicit form of the constants  $A_{2i+1}$  and  $B_{2i+1}$  is too cumbersome to be given here, and will be left out. The energy  $E_n$  for an ATQW is determined from the following secular equation:

$$\begin{aligned} \eta_1(d_1)\eta_1(d_2)\eta_1(d_3) &= \eta_1(d_1)\eta_2(d_2)\eta_2(d_3) \exp[-2\gamma_n b_2] \\ &+ \eta_1(-d_2)\eta_2(d_1)\eta_2(d_3) \exp[-\gamma_n(b_1 + b_2)] \\ &+ \eta_1(d_3)\eta_2(d_1)\eta_2(d_2) \exp[-\gamma_n b_1], \end{aligned} \quad (3)$$

where

$$\eta_1(d) = (1 - \alpha^2) \sin k_n d + 2\alpha \cos k_n d, \quad \eta_2(d) = (1 + \alpha^2) \sin k_n d.$$

As can be observed, for  $b_1 \rightarrow \infty$  and  $b_2 \rightarrow \infty$ , we obtain the secular equation for an uncoupled triple asymmetrical quantum well as follows:

$$\eta_1(d_1)\eta_1(d_2)\eta_1(d_3) = 0,$$

and for  $b_2 \rightarrow \infty$  or  $d_3 \rightarrow 0$  we obtain the equation for two coupled asymmetrical quantum wells:

$$\eta_1(d_1)\eta_1(d_2) = \eta_2(d_1)\eta_2(d_2) \exp[-2\gamma_n b_1]. \quad (4)$$

This equation can also be obtained if we make  $b_1 \rightarrow 0$  or  $d_1 \rightarrow 0$ .

The total energy is given by (see equations (3) and (4))

$$E_n(\mathbf{k}_\perp) = E_n + \frac{\hbar^2}{2m_{1(2)}^*} k_\perp^2 \quad \text{where } E_n = \frac{\hbar^2}{2m_2^*} k_n^2. \quad (5)$$

The physical parameters used for an asymmetrical multiple quantum well of GaAs/Al<sub>0.35</sub>Ga<sub>0.65</sub>As are:  $V_0 = 300$  meV,  $m_1^* = 0.096 m_e$ ,  $m_2^* = 0.0665 m_e$  (where  $m_e$  is the free electron mass). In figure 1, the square of the envelope wavefunction and the energy levels for an asymmetrical double quantum well are presented for the following configurations: (a)  $d_1 = 60$  Å,  $d_2 = 40$  Å,  $b = 10$  Å; and (b)  $d_1 = 60$  Å,  $d_2 = 40$  Å,  $b = 40$  Å. This figure shows that with the increase of the width of the barrier the wavefunction and the energy levels become those of two isolated simple wells of distinct widths, and as the barrier width goes to zero, the energy levels and the probabilities of occupation coincide with those of a single well of width  $d_1 + d_2$ . When the barriers are bigger than 40 Å, the wells are practically uncoupled. When the quantum wells are coupled there exist probabilities for the electron be in either of the two wells, but the probability is greater for one of them. In the case of a symmetrical multiple quantum well, the system remains coupled for barrier widths bigger than 100 Å; also its wavefunctions are symmetrical.

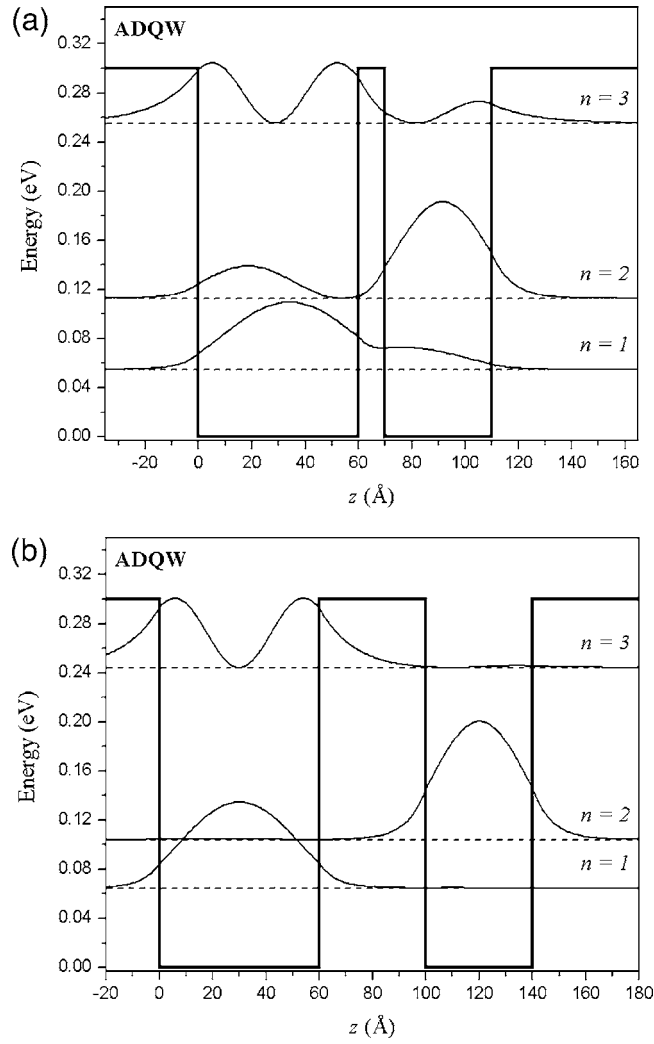


**Figure 1.** Double quantum well with  $d_1 = 60 \text{ \AA}$  and  $d_2 = 40 \text{ \AA}$ : (a)  $b = 10 \text{ \AA}$ , (b)  $b = 40 \text{ \AA}$ .

In figure 2 the energy levels and square of the envelope function for an asymmetrical triple-quantum-well system with widths  $d_1 = 50 \text{ \AA}$ ,  $d_2 = 20 \text{ \AA}$  and  $d_3 = 40 \text{ \AA}$  are shown for the cases (a)  $b_1 = b_2 = 10 \text{ \AA}$  and (b)  $b_1 = b_2 = 40 \text{ \AA}$ . For this case the coupling between wells is weaker than for the double-quantum-well system, due to the number of barriers. However, if we want to obtain a three-energy level system with specific values of the energy, it is theoretically easier or simpler to do this with a triple quantum well than with a double quantum well.

### 3. Electron Raman scattering

The differential cross-section (DCS) per unit solid angle for electron Raman scattering in a volume  $V$  for incident light of frequency  $\omega_l$  and scattered light of frequency  $\omega_s$  is given by [12]

$$\frac{d^2\sigma}{d\omega_s d\Omega} = \frac{V^2 \omega_s^2 \eta(\omega_s)}{8\pi^3 c^4 \eta(\omega_l)} W(\omega_s, \mathbf{e}_s), \quad (6)$$

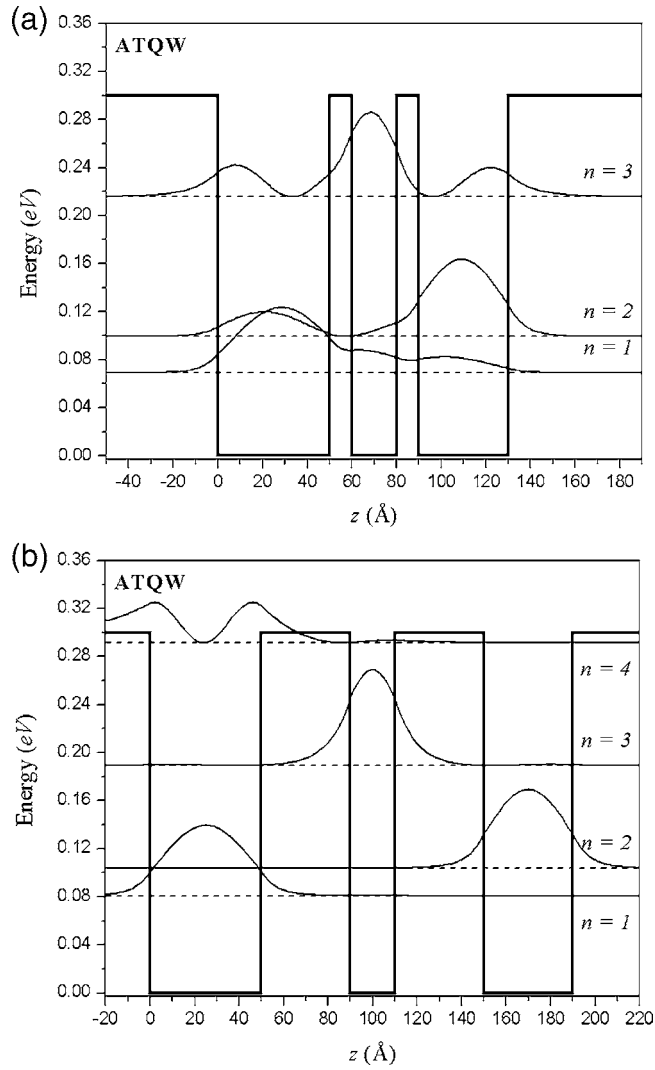


**Figure 2.** Triple quantum well with  $d_1 = 50 \text{ \AA}$ ,  $d_2 = 20 \text{ \AA}$  and  $d_3 = 40 \text{ \AA}$ : (a)  $b_1 = b_2 = 10 \text{ \AA}$ , (b)  $b_1 = b_2 = 40 \text{ \AA}$ .

where  $\eta(\omega)$  is the refraction index as a function of the radiation frequency,  $\mathbf{e}_s(\mathbf{e}_i)$  is the unit polarization vector for the emitted secondary (incident) radiation,  $c$  is the speed of light in vacuum and  $W(\omega_s, \mathbf{e}_s)$  is the transition rate calculated according to Fermi's golden rule:

$$W(\omega_s, \mathbf{e}_s) = \frac{2\pi}{\hbar} \sum_f |M|^2 \delta(E_f - E_i) \quad (7)$$

where  $M$  is calculated in second- or third-order perturbation theory and has the form

$$M_{sl} = \sum_a \frac{\langle b | \hat{H}_s | a \rangle \langle a | \hat{H}_i | i \rangle}{(E_i - E_a + i\Gamma_a)}. \quad (8)$$

$|i\rangle$  and  $|f\rangle$  are the initial and final states corresponding to the energies  $E_i$  and  $E_f$ ,  $|a\rangle$  and  $|b\rangle$  are the intermediate states with energies  $E_a$  and  $E_b$ , and  $\Gamma_a$  and  $\Gamma_b$  are the lifetimes.

The Hamiltonian operator for the radiation field is of the form

$$\hat{H}_r = \frac{|e|\hbar}{m^*} \sqrt{\frac{2\pi\hbar}{V\omega_r}} (\mathbf{e}_r \cdot \hat{\mathbf{p}}), \quad \hat{\mathbf{p}} = -i\hbar\nabla \quad (9)$$

where  $\hat{H}_r$  is in the dipole approximation with frequency  $\omega_r$ ,  $r = l$  ( $s$ ) indicates the incident (secondary) radiation and  $m^*$  is the electron effective mass in the conduction band [12–15].

The effect of reduced dimensionality on the free carrier absorption or emission has been calculated in [16] and the selection rules for intraband and intersubband transitions are shown there. As we can see, the selection rules for a Raman scattering process, given in [16], only allow transitions due to emission or absorption of light if the polarization vector of radiation is in the  $\mathbf{e}_z$  direction.

For the calculation of the differential cross-section given by equation (6) we should evaluate the matrix elements that appear in equation (8). For the case of the radiation field, using equation (9) and the corresponding wavefunctions for asymmetrical multiple quantum wells, the following matrix elements are obtained:

$$\langle \Psi_a | \hat{H}_r | \Psi_b \rangle = \langle \Psi_a | -i\hbar(\mathbf{e}_r \cdot \mathbf{e}_z) \frac{|e|\hbar}{m^*} \sqrt{\frac{2\pi\hbar}{V\omega_r}} \frac{\partial}{\partial z} | \Psi_b \rangle = -i\hbar(\mathbf{e}_r \cdot \mathbf{e}_z) \frac{|e|\hbar}{m^* d_r} \sqrt{\frac{2\pi\hbar}{V\omega_r}} T_{n',n''}(i), \quad (10)$$

where

$$T_{n',n''}(i) = d_r \left( \beta_1 \langle \Psi_a^{\text{outside}} | \frac{\partial}{\partial z} | \Psi_b^{\text{outside}} \rangle + \beta_2 \langle \Psi_a^{\text{inside}} | \frac{\partial}{\partial z} | \Psi_b^{\text{inside}} \rangle \right)$$

and

$$\beta_{1(2)} = \frac{m_0^*}{m_{1(2)}^*}; \quad \frac{1}{m_0^*} = \frac{1}{m_1^*} + \frac{1}{m_2^*}; \quad \frac{1}{d_r} = \sum_i \frac{1}{d_i}.$$

The explicit form of these coefficients is again too cumbersome and therefore will be left out of this discussion.

The Raman differential cross-section for a three-level system is calculated for an ATQW or ADQW, using equation (6).

In the initial state we have an electron in the ground state of the conduction band and a incident photon of energy  $\hbar\omega_l$ , in such a way that (see equation (5))  $E_g = \hbar\omega_l + E_1(\mathbf{k}_\perp)$ . From the ground state the electron carries out a transition to the second intermediate state with energy  $E_u = E_3(\mathbf{k}'_\perp)$ .

From the second intermediate state the electron undergoes a transition toward the first excited state, emitting the laser radiation as secondary radiation of energy  $\hbar\omega_s$ ; thus  $E_l = \hbar\omega_s + E_2(\mathbf{k}''_\perp)$ .

After a number of operations we can write the cross-section as

$$\left[ \frac{d^2\sigma}{d\Omega d\omega_s} \right]_i = \sigma_0 \frac{\omega_s}{\omega_l} |M_0(i)|^2 \frac{E_0^2}{[\hbar\omega_l - \hbar\omega_s + E_1 - E_2]^2 + \Gamma_f^2},$$

where

$$M_0(i) = E_0 \frac{T_{2,3}(i)T_{3,1}(i)}{\hbar\omega_s + E_2 - E_3 + i\Gamma_a}, \quad \sigma_0 = \frac{4e^4\eta(\omega_s)\hbar\Gamma_f}{\pi m_0^{*2} c^4 \eta(\omega_l) E_0^2} |(\mathbf{e}_l \cdot \mathbf{e}_z)(\mathbf{e}_s \cdot \mathbf{e}_z)|^2,$$

$$E_0 = \frac{\hbar^2}{2m_0^* d_r^2}.$$

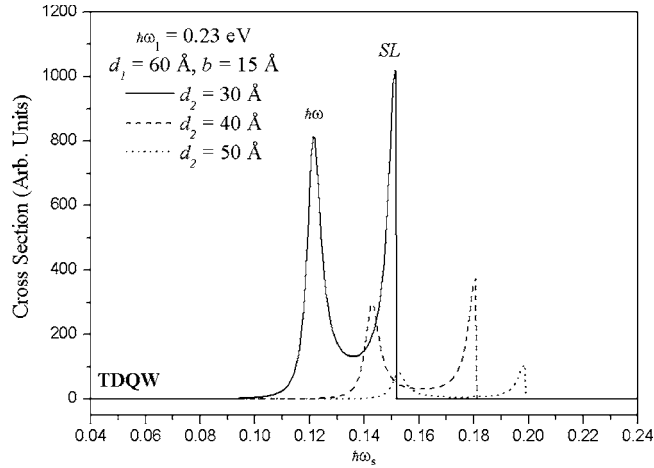


Figure 3. Raman laser cross-section for an ADQW with different widths of the second well.

Finally, we computed the scattering efficiency for emission spectra of the electron Raman laser scattering process. The lifetimes of the final and intermediate states are  $\Gamma_a = \Gamma_f = 3$  meV.

The scattering efficiency has two peaks, a resonant one ( $\hbar\omega$ ) and a non-resonant one (SL: step-like), which are located in  $\hbar\omega = E_3 - E_2$  and  $SL = \hbar\omega_l + E_1 - E_2$ . The resonant peak can only be observed if the incident radiation energy is such that the electron can reach  $E_3$ ; however, for the other peak we only require that the incident radiation be such that the electron reaches  $E_2$ .

In figure 3 the emission spectra of the asymmetrical double quantum well with incident radiation energy  $\hbar\omega_l = 0.23$  eV, width of the first well  $d_1 = 60$  Å, width of the barrier  $b = 10$  Å and three different widths of the second well  $d_2 = 30, 40$  and  $50$  Å are shown. For these spectra we can appreciate that for bigger widths, a displacement of peaks toward bigger energies occurs and with the increase of the width of the second well the efficiency diminishes.

Figure 4 shows the Raman laser cross-section for different widths of the barriers: (a) double quantum well; (b) triple quantum well. In figure 4(a) we can see that an increase of the barrier width in the double quantum well only changes the position of the non-resonant peak, which is due to the  $E_2$  and  $E_3$  levels changing by practically the same amount. In figure 4(b) we can see that the increase of the barrier widths in the triple quantum well changes the position of the two peaks, which is due to  $E_2$  increasing and  $E_3$  diminishing.

In figure 5 the emission spectra for an asymmetrical triple quantum well are shown. In this figure the well widths,  $d_1$  and  $d_3$ , and the barrier widths are kept fixed and three different values of the second well width,  $d_2$ , are taken, which permits us to adjust the secondary-radiation frequency. The behaviour of this figure is very similar to that obtained for the asymmetrical double quantum well; however, the efficiency is smaller, due to this one having two barriers.

#### 4. The net Raman gain of the asymmetrical multiple quantum wells

We have obtained that for a three-energy-level system, like asymmetrical double and triple quantum wells, if the energy levels are ordered according to the numbers  $n_1 = 1$ ,  $n_2 = 2$  and  $n_3 = 3$ , the incident and secondary energies are given by

$$\hbar\omega_s = E_3 - E_2 \quad \text{and} \quad \hbar\omega_l = E_3 - E_1;$$



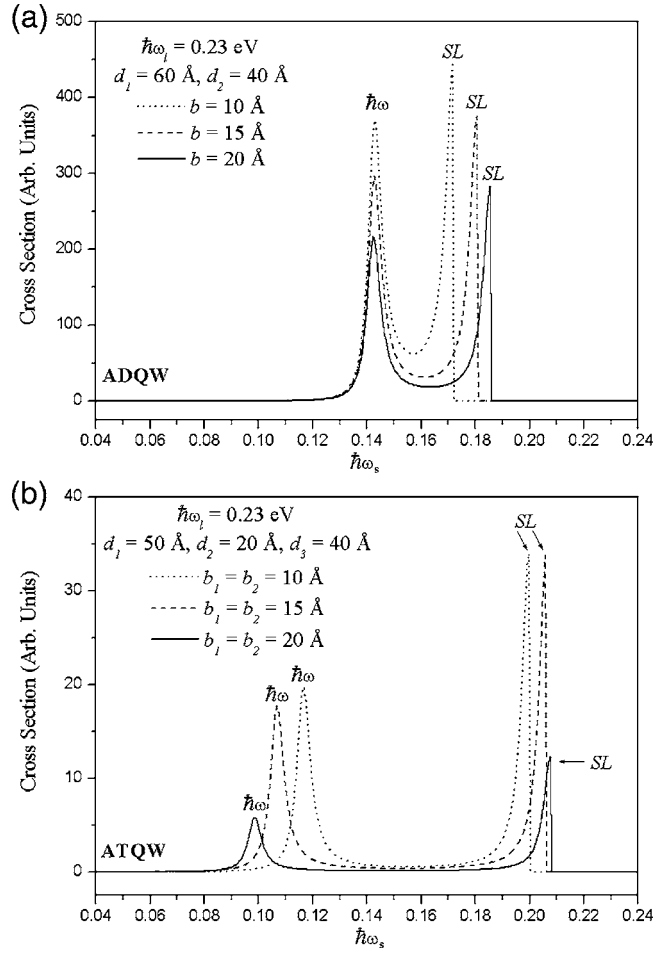


**Figure 4.** Raman laser cross-section for quantum wells with different barrier widths: (a) double quantum well; (b) triple quantum well.

then,

$$\hbar\omega_l - \hbar\omega_s = E_2 - E_1.$$

If the energy of the incident radiation (optical pumping) is below resonance, this difference is named detuning; then, taking into account the detuning  $\delta$  of [2], defined as

$$\delta = E_3 - E_1 - \hbar\omega_l,$$

we have

$$E_3 - E_2 = \hbar\omega_s + \delta \quad \text{and} \quad E_2 - E_1 = \hbar\omega_l - \hbar\omega_s.$$

The expression for the net Raman gain is defined in [2] and it involves the refractive index, the optical pump intensity at frequency  $\omega_l$ , the line broadening, the population densities for the electron states and lifetimes of the states, among other quantities.

In figure 6(a) the net Raman gain for the ADQW is plotted versus the barrier widths, for three different widths of the second well. The gain obtained is similar to the result reported in [2] (the authors used the transfer matrix method). In the figure it can be observed that with

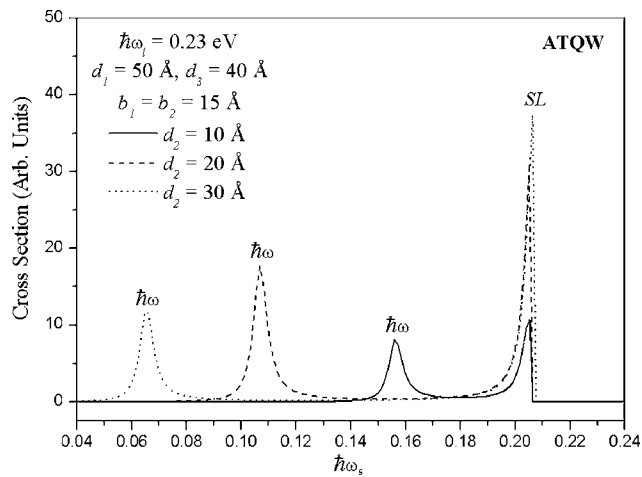


Figure 5. Raman laser cross-section for a triple quantum well with different widths of the second well.

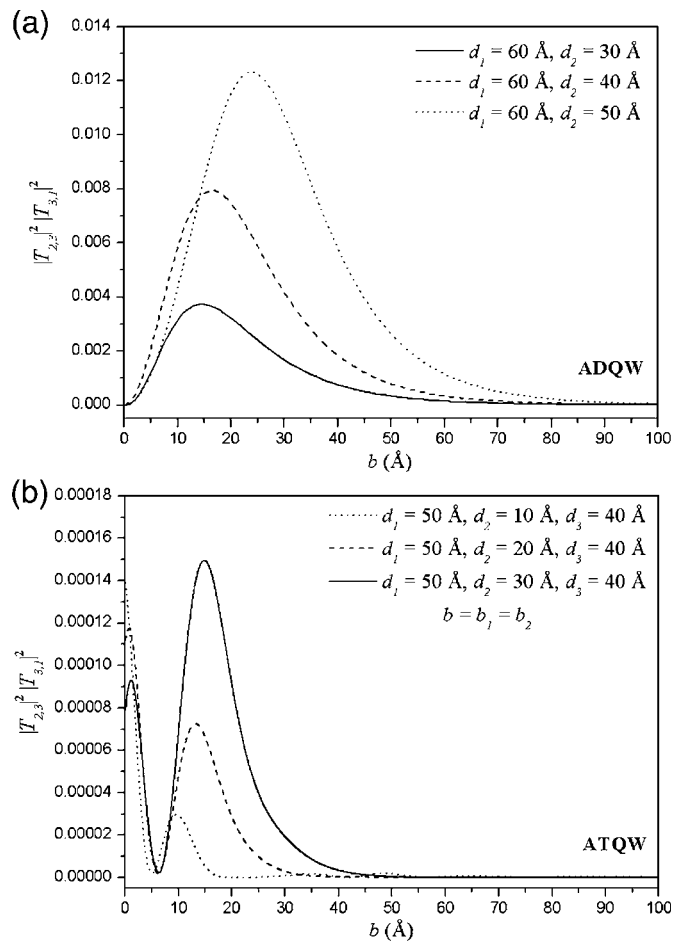
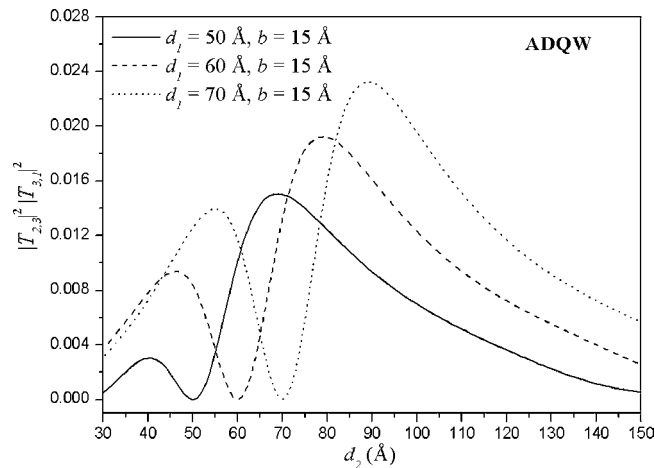


Figure 6. The gain for different barrier widths: (a) for an ADQW, (b) for an ATQW.



**Figure 7.** The gain for different widths of the second well.

the increasing of the width of the second well, the maximum gain is obtained for a bigger barrier. For figure 6(b) the gain for the ATQW is plotted; the results are similar to those obtained in figure 6(a). However, in figure 6(b) two maximum gain peaks appear, which is due to the fact that in this case we have three wells and two barriers. The second peak is the same as that appearing for the ADQW and the first peak is due to the effect of the third well.

Figure 7 shows the net Raman gain for three different widths of the first well with the same barriers versus the second well width for the ADQW. This behaviour accords with the results obtained in the other figures. However, we can note that when the widths coincide,  $d_1 = d_2$ , the wells are symmetric and the gain is zero; it can also be observed that there are two peaks; the first one is when  $d_1 > d_2$ , and the second one is when  $d_1 < d_2$ . This behaviour is due to the fact that the transitions between states with the same parity are forbidden in a symmetrical double couple quantum well.

## 5. Conclusion

In this work we have studied intersubband Raman scattering for a three-level system in a multiple quantum well, specifically for double and triple asymmetrical quantum wells. For this purpose, we use two different methods, obtaining similar results.

Taking into account the results obtained in the present work, we can say that for building a tunable intersubband Raman laser based on multiple quantum wells it is theoretically more efficient to use an asymmetrical double quantum well rather than an asymmetrical triple quantum well; however, from the theoretical point of view, in an asymmetrical triple quantum well it is easier to obtain and optimize the laser radiation frequency.

## Acknowledgments

This work was supported by CONACyT under project number 40629-F. Ivan Marín-Enriquez is currently a student in the PhD programme in Departamento de Investigación en Física, Universidad de Sonora.

## References

- [1] Khurgin J B, Sun G, Friedman L R and Soref R A 1995 *J. Appl. Phys.* **78** 7398
- [2] Sun G, Khurgin J B, Friedman L and Soref R A 1998 *J. Opt. Soc. Am. B* **15** 648
- [3] Liu H C, Cheung I W, SpringThorpe A J, Dharma-Wardana C, Wasilewski Z R, Lockwood D J and Aers G C 2001 *Appl. Phys. Lett.* **78** 3580
- [4] Liu A S and Ning C Z 1999 *Appl. Phys. Lett.* **75** 1207
- [5] Faist J, Capasso F, Sirtori C, Sivco D L, Hutchinson A L and Cho A Y 1995 *Appl. Phys. Lett.* **67** 3057
- [6] Gauthier-Lafaye O, Boucaud P, Julien F H, Sauvage S, Cabaret S, Lourtioz J M, Thierry-Mieg V and Paniel R 1997 *Appl. Phys. Lett.* **71** 3619
- [7] Gmachl C, Belyanin A, Sivco D L, Peabody M L, Owschimikow N, Segent A M, Capasso F and Cho A Y 2003 *IEEE J. Quantum Electron.* **39** 1345
- [8] Jusserand B and Cardona M 1989 *Light Scattering in Solids V (Springer Topics in Applied Physics* vol 66) ed M Cardona and G Güntherodt (Heidelberg: Springer)
- [9] Cardona M 1990 *Superlatt. Microstruct.* **7** 183
- [10] Capasso F, Faist J and Sirtori C 1996 *J. Math. Phys.* **37** 4775
- [11] Wu B H, Cao J C and Xia G Q 2003 *J. Appl. Phys.* **94** 5710
- [12] Riera R, Comas F, Trallero-Giner C and Pavlov S T 1988 *Phys. Status Solidi b* **148** 533
- [13] Betancourt-Riera R, Riera R, Rosas R and Marin J L 2003 *Phys. Low-Dimens. Struct.* **1/2** 125
- [14] Bergues J M, Riera R, Comas F and Trallero-Giner C 1995 *J. Phys.: Condens. Matter* **7** 7273
- [15] Bergues J M, Betancourt-Riera R, Riera R and Marin J L 2000 *J. Phys.: Condens. Matter* **12** 7983
- [16] Riera R, Marín J L and Rosas R A 2001 *Optical Properties and Impurity States in Nanostructured Materials (Handbook of Advanced Electronic and Photonic Devices* vol 6) ed H S Nalwa (New York: Academic) chapter 6